Computers and Structures 98-99 (2012) 1–6

Contents lists available at SciVerse ScienceDirect

Computers and Structures

journal homepage: www.elsevier.com/locate/compstruc

Insight into an implicit time integration scheme for structural dynamics

Klaus-Jürgen Bathe *, Gunwoo Noh

Massachusetts Institute of Technology Cambridge, MA 02139, United States

ARTICLE INFO

Article history:
Received 29 November 2011
Accepted 23 January 2012
Available online 25 February 2012

Keywords:
Structural dynamics
Finite elements
Implicit time integration
Trapezoidal rule
Newmark method
Bathe method

ABSTRACT

In Refs. [1,2], an effective implicit time integration scheme was proposed for the finite element solution of nonlinear problems in structural dynamics. Various important attributes were demonstrated. In particular, it was shown that the scheme remains stable, without the use of adjustable parameters, when the commonly used trapezoidal rule results in unstable solutions. In this paper we focus on additional important attributes of the scheme, and specifically on showing that the procedure can also be effective in linear analyses. We give, in comparison to other methods, the spectral radius, period elongation, and amplitude decay of the scheme and study the solution of a simple 'model problem' with a very flexible and stiff response.

© 2012 Elsevier Ltd. All rights reserved.

1. Introduction

A large amount of research has been performed to identify effective time integration schemes for the linear and nonlinear analyses of structures, see for example Refs. [1–9], and the many references therein. For explicit time integration, commonly, the central difference method is used. For implicit time integration, a number of methods have been proposed and of these, the trapezoidal rule and the alpha methods are now most commonly employed [6,8].

Considering linear analysis, as is well known, the trapezoidal rule is unconditionally stable, second-order accurate, and regarding time integration errors, shows no amplitude decay and acceptable period elongation [6]. However, in nonlinear analyses the method may become unstable, in which case the conditions of momentum and energy conservation are clearly not satisfied. For this reason, research has been focused on establishing more effective time integration schemes for cases in which the trapezoidal rule fails.

One approach is to introduce some damping into a time integration method through the use of adjustable parameters, and this approach has been used in the design of the alpha-methods [8]. The undesirable property is then that the parameters have to be selected and acceptable values depend on the characteristics of the problem solved. If the parameters are set inappropriately, large solution errors may result.

Recently, we proposed an implicit time integration scheme that does not involve the setting of any parameters but merely the selection of an appropriate time step size – as is always required in any implicit time integration solution [1,2,6]. The method combines the use of the trapezoidal rule and an Euler backward method, techniques that have been long time available, see for example Ref. [10]. This combination was proposed for first-order systems by Bank et al. [11], but it took an additional two decades before the method was "discovered" and demonstrated to be effective for the solution of the second-order systems of structural dynamics in finite element solutions [1,2]. Of course, the finite element equations display specific properties and the scheme had to be shown to be reliable and effective for such analyses. The reliability of the integration scheme is particularly important in critical large deformation solutions, see e.g. [6,12–14].

Since the publication of the time integration scheme for finite element solutions involving nonlinear large deformations, much additional experience has been gained. As may be expected, the scheme is now widely used for some nonlinear analyses, specifically also in contact solutions, but – as may not be expected – the method can also be effective in linear analyses.

The objective of this paper is to present a study of the method in linear analysis and compare its performance with the trapezoidal rule and two additional members of the Newmark family of methods that may be considered for solution. In the following, we briefly review the basic equations used in Ref. [2], present some basic properties of the time integration method, and then apply the scheme, and the other methods, in the solution of a simple linear 'model problem' to study and illustrate some important and valuable properties of the method.

* Corresponding author.
E-mail address: kjb@mit.edu (K.J. Bathe).

0045-7949/$ - see front matter © 2012 Elsevier Ltd. All rights reserved.
doi:10.1016/j.compstruc.2012.01.009

2. The time integration scheme

In this section we briefly present the basic equations used in the time integration scheme of Ref. [2] and the stability and accuracy properties.

2.1. The basic equations of time integration

The basic equations used in the time integration scheme have been known for a long time, see e.g. Ref. [10]. In the method of Ref. [2], the complete time step Δt is subdivided into two equal sub-steps. For the first sub-step the trapezoidal rule is used and for the second sub-step the 3-point Euler backward method is employed with the resulting equations

$$ {}^{t+\Delta t/2}\underline{\dot{U}} = {}^{t}\underline{\dot{U}} + \left[\frac{\Delta t}{4}\right]({}^{t}\underline{\ddot{U}} + {}^{t+\Delta t/2}\underline{\ddot{U}}) \tag{1} $$

$$ {}^{t+\Delta t/2}\underline{U} = {}^{t}\underline{U} + \left[\frac{\Delta t}{4}\right]({}^{t}\underline{\dot{U}} + {}^{t+\Delta t/2}\underline{\dot{U}}) \tag{2} $$

$$ {}^{t+\Delta t}\underline{\dot{U}} = \frac{1}{\Delta t}{}^{t}\underline{U} - \frac{4}{\Delta t}{}^{t+\Delta t/2}\underline{U} + \frac{3}{\Delta t}{}^{t+\Delta t}\underline{U} \tag{3} $$

$$ {}^{t+\Delta t}\underline{\ddot{U}} = \frac{1}{\Delta t}{}^{t}\underline{\dot{U}} - \frac{4}{\Delta t}{}^{t+\Delta t/2}\underline{\dot{U}} + \frac{3}{\Delta t}{}^{t+\Delta t}\underline{\dot{U}} \tag{4} $$

Considering linear analysis, the structural dynamics equations applied at time $t + \Delta t/2$ and $t + \Delta t$ are

$$ \underline{M}\,{}^{t+\Delta t/2}\underline{\ddot{U}} + \underline{C}\,{}^{t+\Delta t/2}\underline{\dot{U}} + \underline{K}\,{}^{t+\Delta t/2}\underline{U} = {}^{t+\Delta t/2}\underline{R} \tag{5} $$

$$ \underline{M}\,{}^{t+\Delta t}\underline{\ddot{U}} + \underline{C}\,{}^{t+\Delta t}\underline{\dot{U}} + \underline{K}\,{}^{t+\Delta t}\underline{U} = {}^{t+\Delta t}\underline{R} \tag{6} $$

where $\underline{K}$, $\underline{M}$, $\underline{C}$ are the stiffness, mass and damping matrices, $\underline{U}$ denotes the nodal displacements and rotations, and an overdot denotes a time derivative. Using Eqs. (1)–(6), the time-stepping equations become

$$ \underline{\widehat{K}}_1\,{}^{t+\Delta t/2}\underline{U} = \underline{\widehat{R}}_1 \tag{7} $$

$$ \underline{\widehat{K}}_2\,{}^{t+\Delta t}\underline{U} = \underline{\widehat{R}}_2 \tag{8} $$

where

$$ \underline{\widehat{K}}_1 = \frac{16}{\Delta t^2}\underline{M} + \frac{4}{\Delta t}\underline{C} + \underline{K} \tag{9} $$

$$ \underline{\widehat{K}}_2 = \frac{9}{\Delta t^2}\underline{M} + \frac{3}{\Delta t}\underline{C} + \underline{K} \tag{10} $$

$$ \underline{\widehat{R}}_1 = {}^{t+\Delta t/2}\underline{R} + \underline{M}\left(\frac{16}{\Delta t^2}{}^{t}\underline{U} + \frac{8}{\Delta t}{}^{t}\underline{\dot{U}} + {}^{t}\underline{\ddot{U}}\right) + \underline{C}\left(\frac{4}{\Delta t}{}^{t}\underline{U} + {}^{t}\underline{\dot{U}}\right) \tag{11} $$

$$ \underline{\widehat{R}}_2 = {}^{t+\Delta t}\underline{R} + \underline{M}\left(\frac{12}{\Delta t^2}{}^{t+\Delta t/2}\underline{U} - \frac{3}{\Delta t^2}{}^{t}\underline{U} + \frac{4}{\Delta t}{}^{t+\Delta t/2}\underline{\dot{U}} - \frac{1}{\Delta t}{}^{t}\underline{\dot{U}}\right) + \underline{C}\left(\frac{4}{\Delta t}{}^{t+\Delta t/2}\underline{U} - \frac{1}{\Delta t}{}^{t}\underline{U}\right) \tag{12} $$

With the initial conditions corresponding to time 0.0 known, Eqs. (7) and (8) are used successively for each time step to solve for the required solution, over the complete time domain considered.

Of course, this solution requires the selection of a time step Δt, the factorization of the "effective stiffness matrices" defined in Eqs. (9) and (10) prior to the time integration, and the calculation of the effective load vectors and forward-reductions and back-substitutions for each time step [6]. For an effective solution, clearly as large a time step as possible need to be chosen, and this time step size depends on the accuracy properties of the time integration scheme.

Here we should note that in nonlinear analysis, the use of the different effective stiffness matrices when the trapezoidal rule and the Euler backward method are applied does not increase the solution effort because, in any case, Newton–Raphson iterations are used with new tangent stiffness matrices in each iteration. However, in linear analysis, it may be advantageous to use the same effective stiffness matrix in Eqs. (7) and (8) and this is achieved by using instead of $1/2\Delta t$, the value $(2-\sqrt{2})\Delta t$ in splitting the full time step Δt, see Ref. [1]. Hence, in that case, the equilibrium equations are used at time $t + (2-\sqrt{2})\Delta t$ instead of Eq. (5). Of course, then only one factorization of an effective stiffness matrix is required and also, if the matrix can be kept in-core, less memory is needed.

2.2. The stability and accuracy properties

The method is unconditionally stable, hence the time step to be used in the time integration can be chosen with respect to accuracy considerations only.

A stability analysis can be performed as given for other schemes in Refs. [4–6]. This analysis uses the equation

$$ \begin{bmatrix} {}^{t+\Delta t}\ddot{x} \\ {}^{t+\Delta t}\dot{x} \\ {}^{t+\Delta t}x \end{bmatrix} = \mathbf{A}\begin{bmatrix} {}^{t}\ddot{x} \\ {}^{t}\dot{x} \\ {}^{t}x \end{bmatrix} + \mathbf{L_a}\,{}^{t+\Delta t/2}r + \mathbf{L_b}\,{}^{t+\Delta t}r \tag{13} $$

where $\mathbf{A}$, $\mathbf{L}_a$, and $\mathbf{L}_b$ are the integration approximation and load operators, respectively,

$$ \mathbf{A} = \frac{1}{\beta_1\beta_2}\begin{bmatrix} -4\omega\Delta t(24\xi+7\omega\Delta t) & \omega(-288\xi+14\xi\omega^2\Delta t^2-144\omega\Delta t+5\omega^3\Delta t^3+48\xi^2\omega\Delta t) & \omega^2(24\xi\omega\Delta t+19\omega^2\Delta t^2-144) \\ -4\Delta t(-12+\omega^2\Delta t^2) & 144-47\omega^2\Delta t^2-8\xi\omega^3\Delta t^3-24\xi\omega\Delta t & \omega^2\Delta t(-96-24\xi\omega\Delta t+\omega^2\Delta t^2) \\ 4\Delta t^2(7+2\xi\omega\Delta t) & \Delta t(144-5\omega^2\Delta t^2+80\xi\omega\Delta t+16\xi^2\omega^2\Delta t^2) & -19\omega^2\Delta t^2+144+168\xi\omega\Delta t+48\xi^2\omega^2\Delta t^2-2\xi\omega^3\Delta t^3 \end{bmatrix} \tag{14} $$

$$ \mathbf{L_a} = \frac{1}{\beta_1\beta_2}\begin{bmatrix} -4\omega\Delta t(24\xi+7\omega\Delta t) \\ -4\Delta t(-12+\omega^2\Delta t^2) \\ 4\Delta t^2(7+2\xi\omega\Delta t) \end{bmatrix} \tag{15} $$

$$ \mathbf{L_b} = \frac{1}{\beta_2}\begin{bmatrix} 9 \\ 3\Delta t \\ \Delta t^2 \end{bmatrix} \tag{16} $$

$$ \beta_1 = 16 + 8\xi\omega\Delta t + \omega^2\Delta t^2 \tag{17} $$

$$ \beta_2 = 9 + 6\xi\omega\Delta t + \omega^2\Delta t^2 \tag{18} $$

and ω and ξ are the free vibration natural frequency and the damping ratio, respectively.

Of crucial importance is the behavior of the spectral radius $\rho(\mathbf{A})$ as a function of $\Delta t/T$, where $T = 2\pi/\omega$. We give this radius in Fig. 1, and compare it with the radius of the trapezoidal rule, two Newmark schemes, and the Wilson theta and Houbolt methods [6] (although these last two methods are hardly used anymore because the solution errors of period elongation and amplitude decay are in general too large [6]). In the figure, we refer to the method of Refs. [1,2] as the 'Bathe method'.

In the Newmark schemes the equations used are [6]

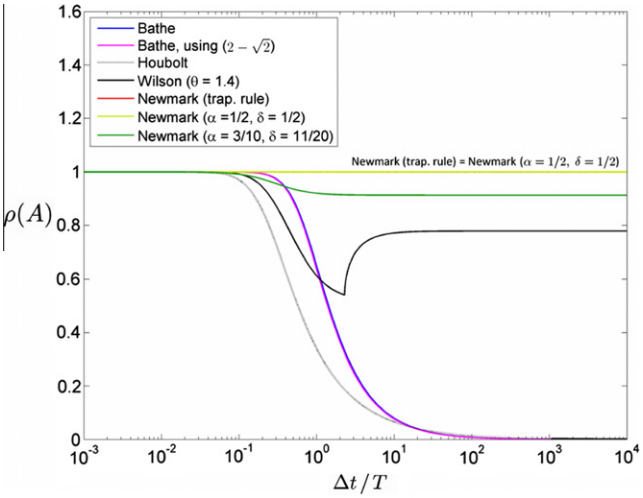

Fig. 1. Spectral radii of approximation operators, case $\xi = 0.0$, for various methods.

$$^{t+\Delta t}\dot{\underline{U}} = {}^{t}\dot{\underline{U}} + [(1-\delta)\,{}^{t}\ddot{\underline{U}} + \delta\,{}^{t+\Delta t}\ddot{\underline{U}}]\Delta t \tag{19}$$

$$^{t+\Delta t}\underline{U} = {}^{t}\underline{U} + {}^{t}\dot{\underline{U}}\Delta t + \left[\left(\frac{1}{2}-\alpha\right){}^{t}\ddot{\underline{U}} + \alpha\,{}^{t+\Delta t}\ddot{\underline{U}}\right]\Delta t^2 \tag{20}$$

where the parameters α and δ employed are given in Fig. 1.

The important point to notice is that in the scheme of Ref. [2] until $\Delta t/T$ is equal to about 0.1 the value of $\rho(\mathbf{A})$ is 1.0 and thereafter it rapidly diminishes. This is a very desirable property because it ensures unconditional stability and, in addition, relates to high accuracy until $\Delta t/T$ is 0.1, with thereafter numerical damping and strong numerical damping in the response for which $\Delta t/T$ is larger than about 0.3. We note that the use of $2-\sqrt{2}$ instead of 1/2 for the splitting of the time step gives practically the same graph of $\rho(\mathbf{A})$.

Figs. 2 and 3 summarize the period elongations and amplitude decays. These results show the accuracy properties of the scheme. The trapezoidal rule has no amplitude decay and an acceptable period elongation. The Bathe method shows a very small amplitude decay and period elongation for reasonable time step values, and when using $\Delta t/T = 0.1$, that is, 10 time steps per period are used, about 14 time steps of the trapezoidal rule result in the same solution error of period elongation. This is an increase of about 40% in solution time using the Bathe method, but the desirable solution quality discussed in Section 3 is obtained.

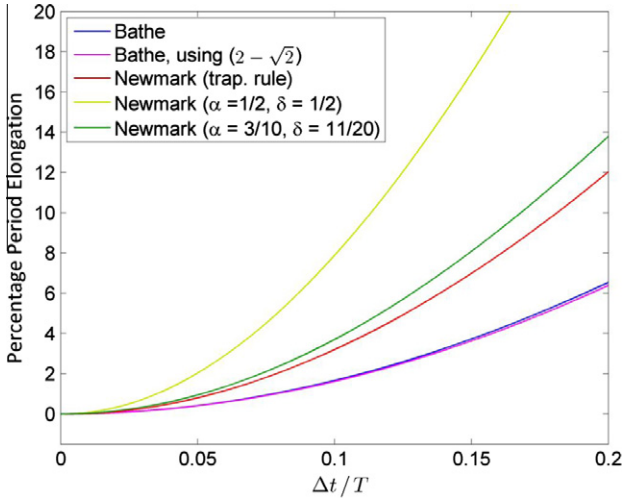

Fig. 2. Percentage period elongations for various methods.

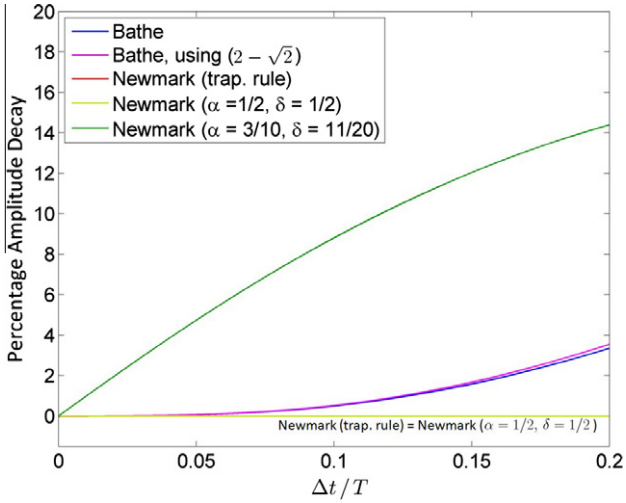

Fig. 3. Percentage amplitude decays for various methods.

Of course, the numerical damping shown in Fig. 3 results into the desired stability in nonlinear solutions [1,2]. We will demonstrate the importance of this damping property in linear analysis in Section 3.

3. A demonstrative solution

Our objective in this section is to present the solution of a simple linear system. The calculated solution yields valuable insight into the properties of the scheme.

We consider the solution of the 3 degree-of-freedom spring system shown in Fig. 4 for which the governing equations are

$$\begin{bmatrix} m_1 & 0 & 0 \\ 0 & m_2 & 0 \\ 0 & 0 & m_3 \end{bmatrix} \begin{bmatrix} \ddot{u}_1 \\ \ddot{u}_2 \\ \ddot{u}_3 \end{bmatrix} + \begin{bmatrix} k_1 & -k_1 & 0 \\ -k_1 & k_1+k_2 & -k_2 \\ 0 & -k_2 & k_2 \end{bmatrix} \begin{bmatrix} u_1 \\ u_2 \\ u_3 \end{bmatrix} = \begin{bmatrix} R_1 \\ 0 \\ 0 \end{bmatrix} \tag{21}$$

For our study we use $k_1 = 10^7$, $k_2 = 1$, $m_1 = 0$, $m_2 = 1$, $m_3 = 1$ and we prescribe the displacement at node 1 to be

$$u_1 = \sin \omega_p t \tag{22}$$

with $\omega_p = 1.2$.

Since node 1 is subjected to the prescribed displacement over time, given in Fig. 4, we rewrite Eq. (21) to solve only for the unknown displacements u_2 and u_3

$$\begin{bmatrix} m_2 & 0 \\ 0 & m_3 \end{bmatrix} \begin{bmatrix} \ddot{u}_2 \\ \ddot{u}_3 \end{bmatrix} + \begin{bmatrix} k_1+k_2 & -k_2 \\ -k_2 & k_2 \end{bmatrix} \begin{bmatrix} u_2 \\ u_3 \end{bmatrix} = \begin{bmatrix} k_1 u_1 \\ 0 \end{bmatrix} \tag{23}$$

after which the reaction is obtained as

$$R_1 = m_1\ddot{u}_1 + k_1 u_1 - k_1 u_2 \tag{24}$$

The important point to note is that we use this simple problem as a 'model problem' to represent the stiff and flexible parts of a much more

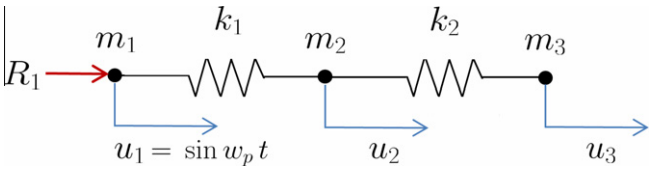

Fig. 4. Model problem of three degrees of freedom spring system, $k_1 = 10^7$, $k_2 = 1$, $m_1 = 0$, $m_2 = 1$, $m_3 = 1$, $\omega_p = 1.2$.

complex structural system. The left high stiffness spring in the model problem is used to represent, for example, almost rigid connections or penalty factors used, while the right flexible spring represents the flexible parts of the complex structural model. The almost rigid (of small flexibility) parts (for example modeled using artificially stiff truss or beam elements) are in the complex model to serve an important purpose but the detailed response *within* these parts is not to be included in the overall system response. Indeed, the high stiffness values used in practice have frequently little physical meaning other than to provide constraints.

In a mode superposition solution, the response within these stiff parts – a response that corresponds to very high artificial frequencies – would naturally not be included.

While in our model problem, of course, the stiff spring could be made infinitely stiff reducing the system to only two degrees of freedom, in practice, we frequently encounter complex finite element models that contain, in essence, such stiff elements in many varied parts of the model and these stiff parts may not be reducible. In fact, we use the system in Fig. 4 as a 'model system' of such complex structural systems of many thousands of degrees of freedom and want to study the behavior of the numerical solution when obtained by the direct integration schemes.

We consider the spring system using zero initial conditions for the displacements and velocities at nodes 2 and 3 (as must typically be done in a complex many degrees of freedom structural analysis), and solve for the response over 10 s. For the solution we use the time stepping schemes for Eq. (23) and also calculate the reaction in Eq. (24). The time step used is $\Delta t = 0.2618$; hence we have $\Delta t/T_p = 0.05$, $\Delta t/T_1 = 0.0417$ and $\Delta t/T_2 = 131.76$, where $T_1 = 6.283$, $T_2 = 0.002$ are the natural periods of the system in Eq. (23) and $T_p = 5.236$ is the period of the prescribed motion at node 1 (some values are rounded).

Figs. 5–13 give the calculated solutions. In these figures we also give the response obtained in a mode superposition solution, referred to as 'reference solution' using only the lowest frequency mode plus the static correction [6] (to do what would typically be done in a practical analysis of a large degree of freedom model).

The figures show that all the time stepping schemes, except the Bathe method, do not perform well, in particular the acceleration at node 2 and the reaction are very poorly predicted. In fact, the trapezoidal rule displays large errors and 'practically' an instability in the calculation of the reaction, see Fig. 12. On the other hand, the Bathe method performs very well – without the adjustment of any parameter. There is only for the first time step an 'undershoot' in Figs. 10 and 13 (which can also be proven analytically to only occur

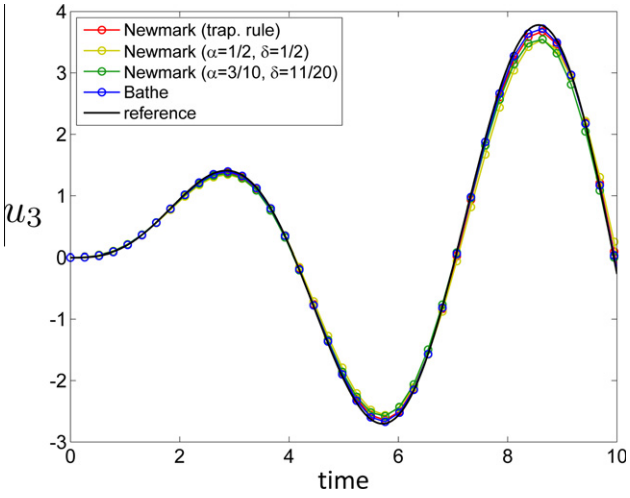

Fig. 6. Displacement of node 3 for various methods.

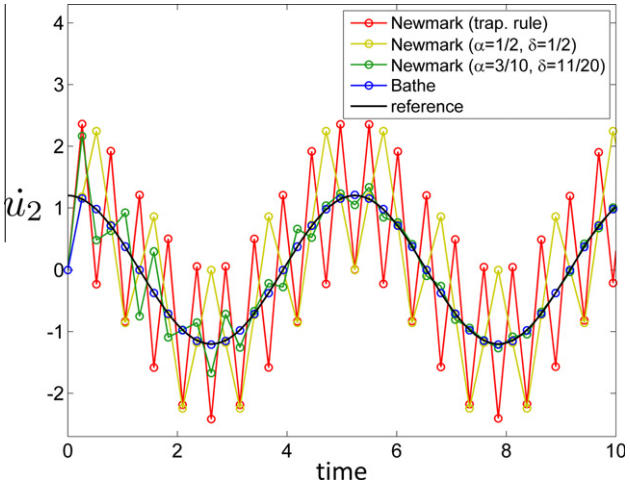

Fig. 7. Velocity of node 2 for various methods (the static correction gives the nonzero velocity at time = 0.0).

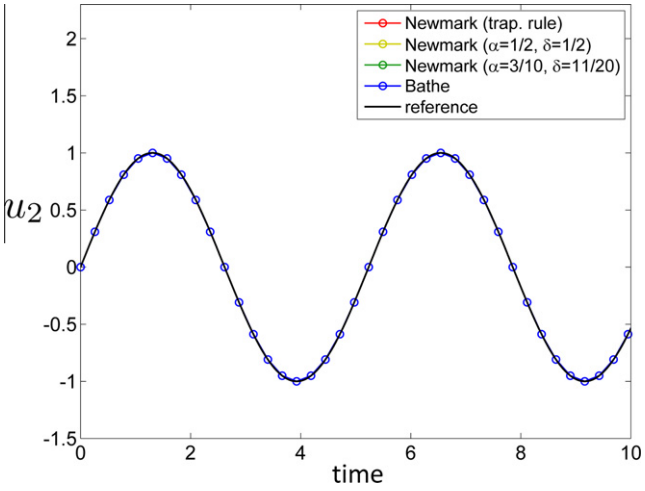

Fig. 5. Displacement of node 2 for various methods.

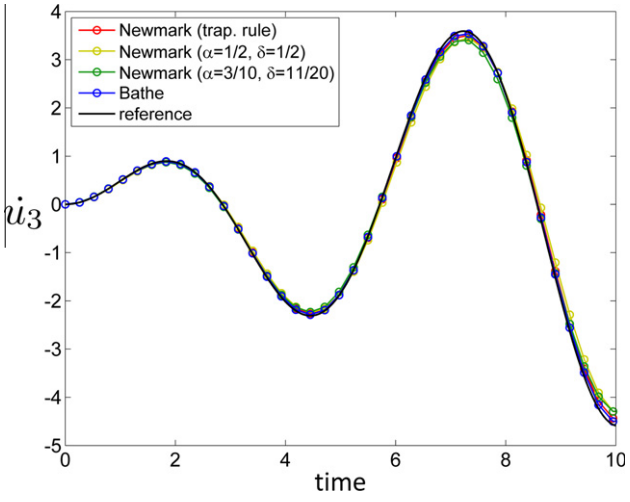

Fig. 8. Velocity of node 3 for various methods.

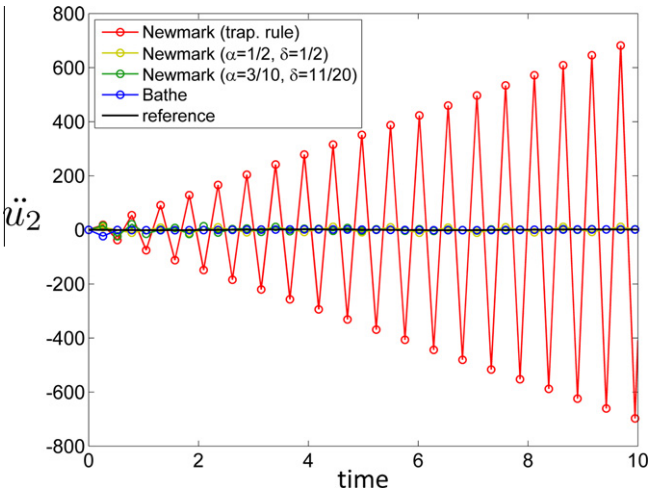

Fig. 9. Acceleration of node 2 for various methods.

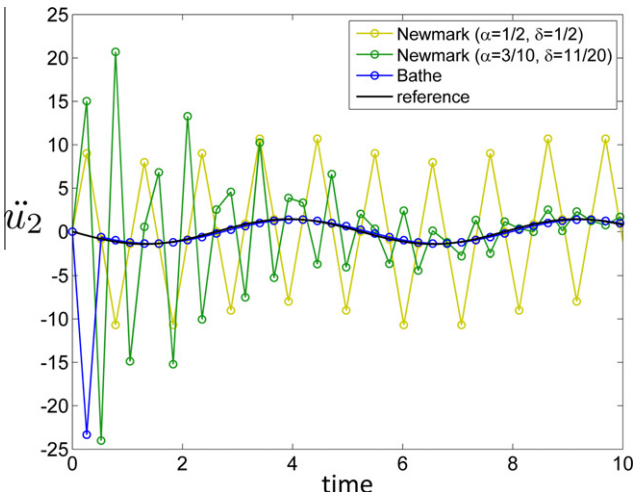

Fig. 10. Acceleration of node 2 for various methods.

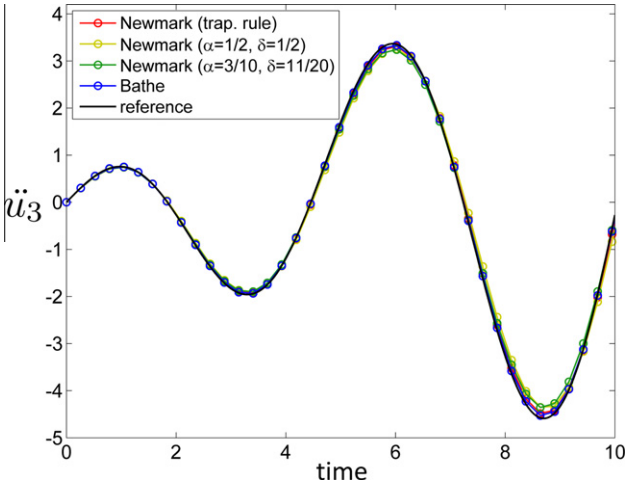

Fig. 11. Acceleration of node 3 for various methods.

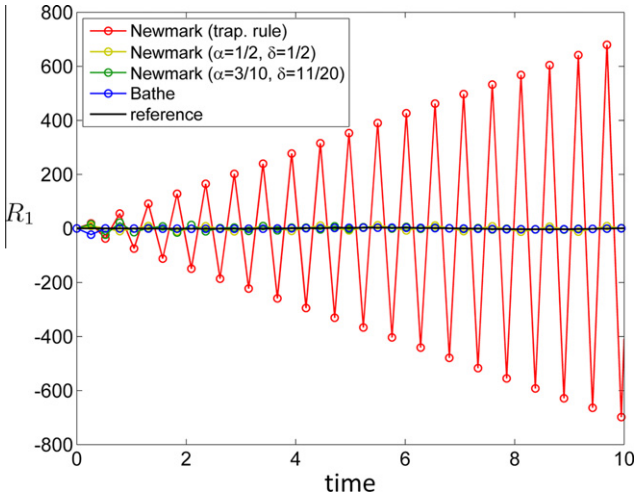

Fig. 12. Reaction force at node 1 for various methods.

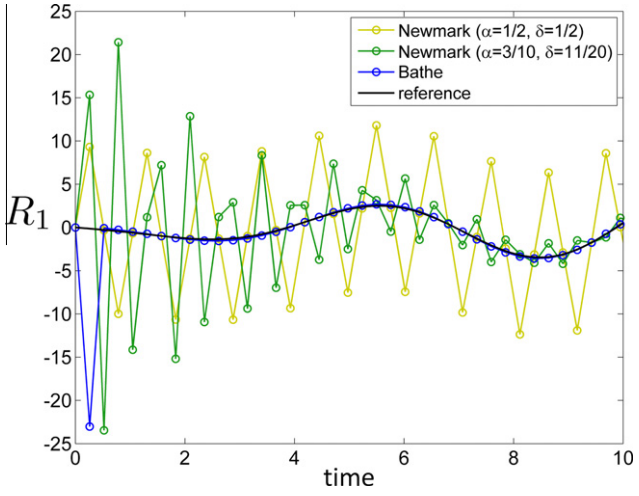

Fig. 13. Reaction force at node 1 for various methods.

in the first step). The important observation is that *the method performs like a mode superposition solution: it calculates the required response accurately and does not include (in essence, discards) the dynamic response in the high frequency mode that is artificial due to modeling*. This fact is very important in practical analyses, and of course holds in linear as well as in nonlinear solutions.

We should note that in this solution $m_1 = 0$. If a nonzero mass is prescribed at the support, the numerical solutions look qualitatively similar.

It is the appropriate numerical damping using the Bathe method that gives a good solution for the velocity and acceleration of node 2, and for the reaction. Of course, numerical damping can be introduced by the use of many methods, for example using the Houbolt and Wilson methods [6], the backward Euler method (Eqs. (3) and (4) applied once or twice per time step), or the Newmark method with specific parameters. Figs. 7, 10 and 13 show that when using the Newmark method with $\alpha = 3/10$ and $\delta = 11/20$ the response is damped and reasonable accuracy is obtained after some solution time. However, the percentage period elongations and amplitude decays of these methods are quite large for reasonable time step ratios.

While we considered here a simple model problem to focus on the essence of the phenomenon studied, the same observations are

made when solving large finite element models in practical engineering and the sciences.

4. Concluding remarks

The objective of this paper was to give some insight into the use of an implicit time integration scheme for the transient response solution of structural, i.e. finite element, systems. While the method proposed in Refs. [1,2] was therein shown to be effective for certain nonlinear analyses, we focused in this paper on the *linear* analysis of structural systems (but the conclusions reached are also valid in nonlinear analysis).

In practice, finite element systems frequently contain very flexible and quite stiff parts (that indeed may only model constraints). In the direct time integration solution, an appropriate time step is chosen and then the solution is marched out for *all* coupled degrees of freedom over the complete time domain considered.

In this paper we studied characteristics and the performance of the method given in Refs. [1,2] referred to herein as the 'Bathe method'. In particular, we considered a simple two degree of freedom 'model problem' to represent the essence of such complex flexible/ stiff systems and to study the response calculated using the trapezoidal rule, two other direct time integration schemes from the Newmark family of methods, and the Bathe method.

This method shows very desirable solution characteristics in that the artificial high frequency response is damped out and not included as errors in the solution. In essence, the response was obtained like in a mode superposition analysis: only the physical mode that is excited is accurately included in the response together with the static correction.

The other methods used, and in particular the trapezoidal rule, did not perform well. In one of the Newmark schemes used, also numerical damping is included but the solution errors are large.

While we deliberately did not include in our study time integration techniques for which numerical parameters need to be chosen – like, for example, the alpha-method [8] – there may of course be other time integration procedures that warrant a study of the kind we have given here. For such study, the simple 'model problem' considered in this paper should be of value.

References

[1] Bathe KJ, Baig MMI. On a composite implicit time integration procedure for nonlinear dynamics. Comput Struct 2005;83:2513–34.
[2] Bathe KJ. Conserving energy and momentum in nonlinear dynamics: a simple implicit time integration scheme. Comput Struct 2007;85:437–45.
[3] Wilson EL, Farhoomand I, Bathe KJ. Nonlinear dynamic analysis of complex structures. Int J Earthquake Eng Struct Dyn 1973;1:241–52.
[4] Bathe KJ, Wilson EL. Stability and accuracy analysis of direct integration methods. Int J Earthquake Eng Struct Dyn 1973;1:283–91.
[5] Tedesco JW, McDougal WG, Ross CA. Structural dynamics, theory and applications. Addison–Wesley; 1998.
[6] Bathe KJ. Finite element procedures. Prentice Hall; 1996.
[7] Simo JC, Tarnow N. The discrete energy-momentum method. Conserving algorithms for nonlinear elastodynamics. J Appl Math Phys 1992;43:757–92.
[8] Chung J, Hulbert GM. A time integration algorithm for structural dynamics with improved numerical dissipation: the generalized alpha method. J Appl Mech Trans ASME 1993;60:371–5.
[9] Masuri SU, Hoitink A, Zhou X, Tamma KK. Algorithms by design: a new normalized time-weighted residual methodology and design of a family of energy-momentum conserving algorithms for non-linear structural dynamics. Int J Numer Methods Eng 2009;79:1094–146.
[10] Collatz L. The numerical treatment of differential equations. 3rd ed. Springer-Verlag; 1966.
[11] Bank RE, Coughran WM, Fichtner W, Grosse EH, Rose DJ, Smith RK. Transient simulation of silicon devices and circuits. IEEE Trans CAD 1985;4:436–51.
[12] Bathe KJ. On reliable finite element methods for extreme loading conditions. In: Ibrahimbegovic A, Kozar I, editors. Chapter in extreme man-made and natural hazards in dynamics of structures. Springer-Verlag; 2007.
[13] Kazanci Z, Bathe KJ. Crushing and crashing of tubes with implicit time integration. Int J Impact Eng 2012;42:80–8.
[14] Bathe KJ. The finite element method. In: Wah B, editor. Encyclopedia of computer science and engineering. John Wiley and Sons; 2009. p. 1253–64.